PHYSICAL REVIEW A VOLUME 10, NUMBER 1 JULY 1974

Propagation of sound in water. A molecular-dynamics study*

Aneesur Rahman
Argonne National Laboratory, Argonne, Illinois 60439

Frank H. Stillinger
Bell Laboratories, Murray Hill, New Jersey 07974
(Received 25 March 1974)

Fluctuation phenomena occurring in a system of 216 water molecules, studied by molecular dynamics at 1 g cm^{-3} and 10 °C, indicate that (i) transverse currents persist in the form of propagating collective coordinates even for a wavelength of about 20 Å, with indications that the same will happen for much longer wavelengths. The velocity of propagation is 1.05×10^5 cm sec^{-1}. In the region of 20 Å the lifetime of the fluctuation appears to increase *linearly* with increasing wavelength. (ii) Density fluctuations at 20 Å are found to be propagating but only marginally; the corresponding velocity of sound is 1.8×10^5 cm sec^{-1}. (iii) The spectrum of density fluctuations exhibits a secondary maximum at a much higher frequency than the normal frequency of sound propagation and it is suggested that experiments should be directed to the region of this "high-frequency sound."

I. INTRODUCTION

In recent years we have reported the results of molecular-dynamics (MD) studies of the structure of water and of the motions of molecules in that liquid. An initial study[1] showed that it was feasible and fruitful to undertake such calculations on the basis of an "effective" noncentral pair interaction that produces a computer liquid with properties similar to those real water is known to possess. However, the discrepancy between the calculated and the observed structure of the liquid was such as to motivate an improved simulation with appropriate modifications in the potential. The results of this improved simulation were indeed very encouraging[2,3] as far as the structure was concerned, and hence we have undertaken a detailed analysis of the dynamical properties of the computer liquid. One such study has already been reported[4]; it concerns the motion of protons as they are carried around by the parent molecules which translate and rotate in concert with and hindered by the neighboring molecules. This study of proton motions is of interest to the experimental technique of neutron inelastic scattering; in the case of H_2O the cross section of such scattering is in large measure determined by the motion of protons alone.

In this report we present the analysis of fluctuations in density and in transverse currents in the liquid. Several such studies of monatomic liquids have already been made and have led to the accumulation of a wealth of information regarding the space-time characteristics of these fluctuations for short wavelengths. Theoretical interpretation of these results for monatomic liquids has deepened the understanding of the nature of these fluctuations. Water differs from simple monatomic liquids in that the immediate neighborhood of a molecule is far from being "well packed"; each molecule has only about four to five near neighbors with very strong bonds which resist change of shape as well as of volume of the local structure. Hence, for short wavelength disturbances, the behavior of this strongly bonded liquid is expected to pose new problems in the understanding of fluctuation of density and transverse currents. We hope that the results presented here will be of help in this development.

Section II is devoted to formal definitions of the various collective coordinates to be dealt with in this report. Some of the basic properties have been stated; the notation is essentially the same as that used in an analysis of fluctuation phenomena in liquid sodium made by one of us.[5]

In Sec. III the essential elements of the molecular-dynamics calculation on water have been summarized. For further details one should use Ref. 2. We have also given a brief outline of the manner in which space-time data generated in a molecular-dynamics run are Fourier transformed to give wave-number–time behavior of various collective coordinates.

The time behavior of the collective coordinates is presented in Sec. IV; already at this stage, before further analysis, one sees that transverse currents in our water model show a certain persistence which is absent in the results obtained for monatomic systems.

Sections V and VI are devoted to a spectral analysis of transverse and longitudinal currents, respectively. In the latter case the memory-func-

tion approach has been used as an extrapolation device to extend the data to times longer than those attained by the molecular-dynamics calculation.

Finally, in Sec. VII the results of this analysis are discussed in terms of existing experimental data on water and in terms of experiments that might be performed in the light of these results. The results of a dynamical-matrix analysis on single crystals of ice are also mentioned in Sec. VII, as well as the experimental data on sound propagation in polycrystalline ice.

II. DEFINITIONS AND FORMAL CONSIDERATIONS

Let $\vec{r}_j, \vec{v}_j$ denote the position and velocity of the center of mass of molecule j in the liquid consisting of N molecules, each having mass M.

The density at $\vec{r}$ at time t is defined as

$$\rho(\vec{r}, t) = \sum_{j=1}^{N} \delta(\vec{r} - \vec{r}_j(t)) \; ; \tag{1}$$

its Fourier component for wave vector $\vec{\kappa}$ is then

$$Q(\vec{\kappa}, t) = N^{-1/2} \sum e^{i\vec{\kappa}\cdot\vec{r}_j(t)} \; . \tag{2}$$

Normalization with $N^{-1/2}$ is a matter of later convenience. The density fluctuation for the wave vector with magnitude $\kappa = |\vec{\kappa}|$ is defined as

$$F(\kappa, t) = \langle Q(\vec{\kappa}, s) Q^*(\vec{\kappa}, s+t) \rangle \; , \tag{3}$$

where $\langle \cdots \rangle$ is an average over initial conditions s and over the directions of vectors $\vec{\kappa}$ of magnitude κ. Of course, it is assumed that the system is in dynamic equilibrium at temperature T. The frequency spectrum, $S(\kappa, \omega)$ of density fluctuations is defined as

$$S(\kappa, \omega) = \frac{1}{2\pi} \int_{-\infty}^{+\infty} F(\kappa, t) e^{i\omega t} \, dt \; . \tag{4}$$

Starting with the velocity current density,

$$\vec{J}(\vec{\kappa}, t) = N^{-1/2} \sum \vec{v}_j(t) e^{i\vec{\kappa}\cdot\vec{r}_j(t)} \; , \tag{5}$$

we define two correlations, $C_\parallel$ and $C_\perp$:

$$C_\parallel(\kappa, t) = \langle J_\parallel(\vec{\kappa}, s) J_\parallel^*(\vec{\kappa}, s+t) \rangle \; ; \tag{6}$$

$$C_\perp(\kappa, t) = \langle J_\perp(\vec{\kappa}, s) J_\perp^*(\vec{\kappa}, s+t) \rangle \; . \tag{7}$$

In Eq. (6) $J_\parallel$ stands for $\kappa^{-1}(\vec{\kappa}\cdot\vec{J})$ and in Eq. (7) $J_\perp$ is written for a component of $\vec{J}$ normal to $\vec{\kappa}$. Analogous to Eq. (4), the spectra of $C_\parallel$ and $C_\perp$ are denoted by $\tilde{C}_\parallel(\kappa, \omega)$ and $\tilde{C}_\perp(\kappa, \omega)$, respectively. Using

$$\frac{d}{dt} Q(\vec{\kappa}, t) = i\kappa J_\parallel(\vec{\kappa}, t) \, , \tag{7'}$$

it is easy to show that

$$\kappa^2 C_\parallel(\kappa, t) = -\frac{d^2}{dt^2} F(\kappa, t) \, , \tag{8}$$

$$\kappa^2 \tilde{C}_\parallel(\kappa, \omega) = \omega^2 S(\kappa, \omega) \, . \tag{9}$$

However, $\tilde{C}_\perp$ is in no obvious way related to $S(\kappa, \omega)$.

Assuming throughout that we are dealing with a system obeying the laws of classical statistical mechanics and that it is in equilibrium, it follows that all time correlations defined above are even functions of time and consequently the spectra are simply the cosine transforms of the respective time correlations. For the spectrum $S(\kappa, \omega)$, we shall write

$$\langle \omega^n \rangle = \int_{-\infty}^{+\infty} \omega^n S(\kappa, \omega) \, d\omega \tag{10}$$

for the nth frequency moment, which of course depends on n and on κ. Under the assumption just mentioned, all the odd moments of $S(\kappa, \omega)$ are zero.

Some essential formal properties of the various functions defined above will now be given:

$$S(\kappa) \equiv F(\kappa, 0) = \left\langle N^{-1} \sum \sum \exp\{i\vec{\kappa}\cdot[\vec{r}_l(s) - \vec{r}_j(s)]\} \right\rangle \tag{11}$$

represents the space Fourier transform of the instantaneous pair structure of the system; it is usually referred to as the structure factor. It is easy to see that

$$\langle \omega^0 \rangle = S(\kappa); \tag{12}$$

$$\langle \omega^2 \rangle = \kappa^2 k_B T / M = \kappa^2 C_\parallel(\kappa, t=0) \, . \tag{13}$$

We shall write the Taylor-series expansion of $F(\kappa, t)$ as

$$F(\kappa, t) = S(\kappa)(1 - \omega_0^2 t^2/2! + \omega_0^2 \omega_l^2 t^4/4! \ldots) \, , \tag{14}$$

where $\omega_0^2 = \kappa^2 k_B T / M S(\kappa) = \langle \omega^2 \rangle / \langle \omega^0 \rangle$ and $\omega_l^2 = \langle \omega^4 \rangle / \langle \omega^2 \rangle$. From Eq. (8) it follows that

$$C_\parallel(\kappa, t) = k_B T / M (1 - \omega_l^2 t^2/2! + \ldots) \, . \tag{15}$$

Similarly, we write

$$C_\perp(\kappa, t) = k_B T / M (1 - \omega_t^2 t^2/2! + \ldots) \, . \tag{16}$$

The suffixes l and t in ω_l^2, ω_t^2 stand for longitudinal and transverse, respectively.

One can express ω_l^2, ω_t^2 in terms of the potential and the pair-correlation function only in the special case of monatomic systems with pair interactions.[6,7] Moreover, for the special case mentioned, ω_l^2 and ω_t^2 are simply related to the infinite frequency elastic moduli.[6,7] No such simple relation seems to exist in the general case.

Equation (9) shows that $\tilde{C}_{\parallel}(\kappa, \omega=0)=0$; this is a direct consequence of the conservation equation: $\dot{Q}=i\kappa J_{\parallel}$, Eq. (7′). However, $\tilde{C}_{\perp}(\kappa, \omega=0)$ in general does not vanish.

In the limit of long wavelength, i.e., as $\kappa \to 0$, $S(\kappa) \to nk_BT\chi_T = k_BT/Mc_T^2$, where n is the number density, χ_T is the isothermal compressibility, and c_T is the isothermal sound velocity. In the limit $\kappa \to 0$, $S(\kappa, \omega)$ is expected to show the three-line phenomenon, i.e., the spectrum is concentrated sharply around $\omega=0$ and $\omega=\pm \kappa c_s$, where c_s is the adiabatic sound velocity; the widths of the three lines are determined by viscosity and heat conductivity. In other words, for long wavelengths one has propagating density fluctuations with rather long lifetimes. For extremely short wavelengths ($\kappa \to \infty$) these are over-damped fluctuations which do not propagate. The central question, to be answered by the method of molecular dynamics, concerns the behavior of density fluctuations for wavelengths comparable to the distance between neighboring particles in the liquid.

For transverse currents the situation is different. As $\lambda \to \infty$ ($\kappa \to 0$) a liquid is unable to propagate shear waves so that $\tilde{C}_{\perp}(\kappa, \omega)$ exhibits a maximum at $\omega=0$, and no recognizable nonzero frequency of propagation [analogous to $\omega=\pm \kappa c_s$ for $\tilde{C}_{\parallel}(\kappa, \omega)$]. However, for shorter wavelengths the behavior is not obvious and molecular dynamics is in fact the *only* method known that can throw light on this question.

III. MOLECULAR DYNAMICS OUTLINE

The analysis of density fluctuations being reported here was made from trajectories of water molecules generated in a molecular-dynamics calculation[2] on liquid water in which the total potential energy is written as a sum of effective pair potentials. This potential uses a four-point-charge model for each molecule; the molecule itself is considered to be a rigid structure. Specifically,

$$V(1,2)=V_{LJ}(r_{12})+S(r_{12})V_{el}(1,2),$$

where r_{12} is the oxygen-to-oxygen distance. V_{LJ} is a Lennard-Jones (6, 12) function:

$$V_{LJ}(r)=4\epsilon[(\sigma/r)^{12}-(\sigma/r)^6],$$

with $\epsilon=5.2605\times10^{-15}$ ergs and $\sigma=3.1$ Å. Each molecule has four charges $\pm q$ contributing 16 Coulombic interactions gathered into $V_{el}(1,2)$; $|q|=0.2357e$ or 1.13194×10^{-10} esu. The two $+q$'s are 1 Å from the oxygen at the positions of the two protons. The $-q$'s are 0.8 Å from the oxygen. The four lines joining the oxygen to these charges form precise tetrahedral angles (109°28′) with one another. Finally,

$$S(r)=(r-R_L)^2(3R_U-R_L-2r)/(R_U-R_L)^3$$

for $R_L \leq r \leq R_U$, joining smoothly to the value 0 for $r<R_L$ and to the value 1 for $r>R_U$. The values of R_L and R_U are 2.0160 and 3.1287 Å, respectively.

The molecular-dynamics run[2] was made with 216 water molecules at a density 1 g cm^{-3} and $T=10$ °C. The total time of integration of the equations of motion was $38100\Delta t$, the step Δt being $10^{-4}\tau$, where $\tau=2.126$ psec.

This potential seems to give a moderately good account of the properties of liquid water. Details have been published elsewhere.[2-4]

As in all extensive molecular-dynamics calculations, the trajectories are recorded on magnetic tape. For the present purpose we can refer to this as the $(\vec{r}, t)$ tape which contains a record of positions $\vec{r}_j(t)$ and velocities $\vec{v}_j(t)$ of the centers of mass of all the 216 molecules.

Since the calculation is made on a strictly periodic system in x, y, z, with periodicity interval $L=18.62$ Å, we define a mesh of wave vectors $\vec{\kappa}=(l,m,n)2\pi/L$, where l, m, n are $0, \pm1, \pm2, \ldots$, etc. Using the $(\vec{r}, t)$ tape, one creates its Fourier transform, a $(\vec{\kappa}, t)$ tape. This consists of the values of $Q(\vec{\kappa}, t)$ and $\vec{J}(\vec{\kappa}, t)$ [Eqs. (2) and (3)]. Next, the $(\vec{\kappa}, t)$ tape is used for calculating the autocorrelations $F(\kappa, t)$, $C_{\parallel}(\kappa, t)$, and $C_{\perp}(\kappa, t)$ [Eqs. (3), (6) and (7)]. Finally, the spectra $S(\kappa, \omega)$, $\tilde{C}_{\parallel}(\kappa, \omega)$, and $\tilde{C}_{\perp}(\kappa, \omega)$ are calculated from the autocorrelations.

The smallest nonzero value of κ is $2\pi/L$. For this the $(\vec{\kappa}, t)$ tape contains information with three vectors $\vec{\kappa}$ (note that $-\vec{\kappa}$ does not give new information). Similarly for $\kappa=(2\pi/L)\sqrt{2}$ one has six vectors over which to average. This multiplicity is easily worked out for any triplet l, m, n defining $\vec{\kappa}$ and is involved in the averaging indicated by $\langle \ldots \rangle$ in Eq. (3). For transverse currents the multiplicity is obviously twice as big.

Normalizing the raw data on F, $C_{\parallel}$, and $C_{\perp}$ to unity at $t=0$, the coefficients ω_0^2, ω_t^2, ω_t^2 [Eqs. (14)–(16)] can be evaluated by numerical fitting.

The properties of the Fourier transforms, i.e., the spectral function, will be considered in a later section.

IV. DESCRIPTIVE PRESENTATION OF RESULTS ON TIME CORRELATIONS

In this paper we will be interested in studying wavelengths that are not too short compared to the interparticle separation; hence, calculations were performed only for values of κ up to about

2.5 $Å^{-1}$. The results for the time correlations $F, C_{\parallel}$, and $C_{\perp}$ will now be summarized.

The value of $F(\kappa, t)$ at $t=0$ is the structure factor $S(\kappa)$ [see Eq. (11)] for the positions of the centers of mass. This is shown in Fig. 1. Note that $S(\kappa)$ clearly shows a local maximum at about 2 $Å^{-1}$. We recall[2] that x-ray scattering experiments, which, to a good approximation, can be considered to monitor the positions of the oxygens alone, also show a local maximum at 2 $Å^{-1}$. Since the oxygen is fairly close to the center of mass of the molecule, it would thus appear that the local maximum seen in Fig. 1 has the same structural origin as the one seen in x-ray experiments.

The top part of Fig. 1 shows the values of $C_{\parallel}(\kappa, t)$ and $C_{\perp}(\kappa, t)$ at $t=0$. In principle, these should be k_BT/M, independent of κ; expressing k_BT/M in units of ϵ/M, we get $T^*=k_BT/\epsilon=7.43$ for $T=10°C$. This value is also indicated in the figure. The fluctuation around this value indicates that for κ below about 0.8 $Å^{-1}$, much longer dynamical runs are required to reduce the statistical errors.

Figure 2 displays the time correlations for five values of κ chosen so as to bring out the remarkable change that occurs in going from $\kappa \sim 0.3$ $Å^{-1}$ (or $\lambda \sim 20$ Å) to $\kappa \sim 2.4$ $Å^{-1}$ (or $\lambda \sim 2.5$ Å $\approx$ the first-neighbor distance in the system).

(i) $C_{\perp}(\kappa, t)$: Even at $\kappa \sim 0.3$ $Å^{-1}$, this correlation oscillates around zero as it decays; in a liquid we expect that as $\kappa \to 0$ a transverse current fluctuation will be overdamped because of the inability of the liquid to transmit shear waves of long wavelength. Figure 2 shows that in water, presumably because of the considerable rigidity of the hydrogen-bond network, the system has a certain elastic behavior in response to a shear even at $\lambda \sim 20$ Å. For larger κ, as seen from Fig. 2, the correlation $C_{\perp}(\kappa, t)$ starts to reflect the behavior of the velocity autocorrelation of the center of mass of the individual molecules (see, e.g., Fig. 13 in Ref. 2). The Lennard-Jones liquid molecular dynamics calculations have shown that at $\kappa \sim 0.25$ $Å^{-1}$, $C_{\perp}(\kappa, t)$ has a simple overdamped decay. Thus by comparison[8] the model of liquid water studied here shows a very different behavior at a comparable wavelength.

(ii) $F(\kappa, t)$: For small values of κ the behavior of this function (Fig. 2) indicates an initial fast decay and then a much slower one; in other words, there are two rather disparate time scales involved in the time dependence of $F(\kappa, t)$ at the small values of κ studied here. For large κ, Fig. 2 shows $F(\kappa, t)$ to be a relatively simple decaying function with much less obvious structure.

(iii) $C_{\parallel}(\kappa, t)$: Because of the conservation equation for the number density, the correlation $C_{\parallel}(\kappa, t)$ has zero mean value—in other words, $\tilde{C}_{\parallel}(\kappa, \omega=0)=0$. Since $C_{\parallel}(\kappa, t=0)>0$, sign changes are inherent in $C_{\parallel}(\kappa, t)$. Apart from this obvious property, the behavior of $C_{\parallel}(\kappa, t)$ seen in Fig. 2 does not seem, at first sight, to show any parti-

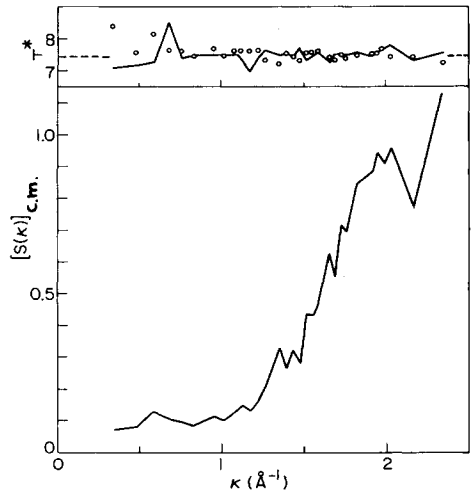

FIG. 1. Structure factor $S(\kappa)$ for center-of-mass positions. The main peak is beyond the region of κ shown. The top part of the figure shows the values of $C_{\parallel}(\kappa, t=0)$ and $C_{\perp}(\kappa, t=0)$; see Eqs. (15) and (16). Temperature of the system (10 °C) is shown with dashes; T^* indicates the temperature in dimensionless units (see Sec. IV).

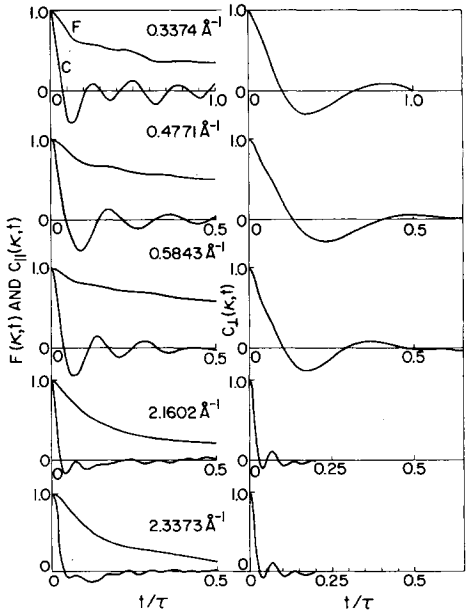

FIG. 2. Overall view of the time correlations investigated. Note that the time scale has been modified appropriately for various values of κ. All correlations have been normalized to unity at $t=0$. The legends should therefore be read as $F(\kappa,t)/F(\kappa,0)$, etc.

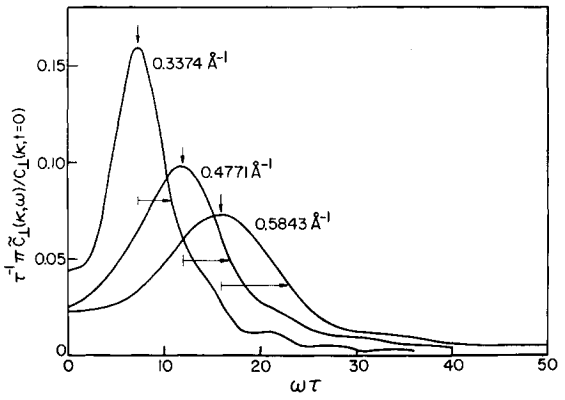

FIG. 3. Spectral functions for transverse currents. It is clear that freely propagating shear waves have a very well-defined frequency of maximum response ω_m (see Fig. 5) and considerable lifetime.

cularly remarkable feature. However, as will be seen later, there is indeed considerable information in the time dependence of $C_{\parallel}(\kappa, t)$ regarding the characteristic propagation of density fluctuations in the water model considered.

V. SPECTRAL ANALYSIS OF TRANSVERSE CURRENTS

A. Propagation of shear waves

The function $\pi\tilde{C}_{\perp}(\kappa, \omega)/C_{\perp}(\kappa, t=0)$ is the one-sided cosine transform of $C_{\perp}(\kappa, t)/C_{\perp}(\kappa, t=0)$.

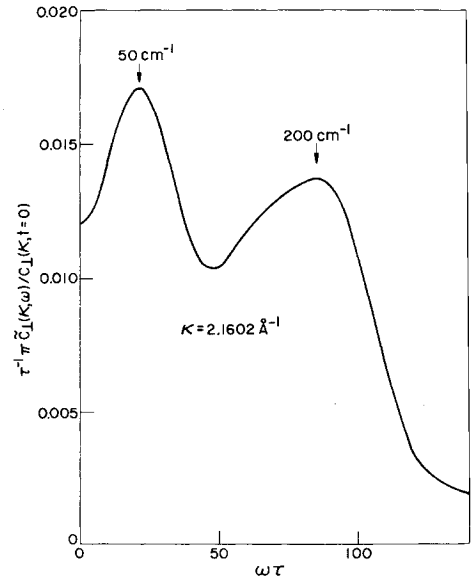

FIG. 4. For large κ transverse current collective coordinate behaves mostly like a single-particle mode. The spectral function shown above is essentially the same as the spectrum of the center-of-mass velocity autocorrelation function (see Fig. 13 in Ref. 2).

It is shown in Fig. 3 for three small values of κ and in Fig. 4 for one large value. From Fig. 3 it is obvious that we have propagating shear waves with a very well-defined velocity of propagation and a not so ill-defined lifetime. On the other hand, in Fig. 4 the spectrum is a wide band extending from $\omega = 0$ to about 50 psec^{-1} (or 250 cm^{-1}); this spectrum is essentially the same as that of the velocity autocorrelation of the center of mass of the molecule (see Fig. 13 in Ref. 2). Thus around $\kappa = 0.3$ Å^{-1} the transverse current describes a well-defined collective coordinate, whereas by the time κ is 2 Å^{-1} it contains information regarding the motion of just single molecules. Even when the collective coordinate is well defined, its time dependence shows some features related to the single-particle motion; the high-frequency part of the spectrum in Fig. 4 can be seen to be present but with very low intensity even for the values of κ shown in Fig. 3; for $\kappa = 0.5843$ Å^{-1}, e.g., there is a clear long tail in the spectrum on the high-frequency side.

In Fig. 5 we have drawn ω_m, the frequency of maximum response, as a function of κ. The two thick arrows on the high-κ side of Fig. 5 represent the positions of the maxima in Fig. 4. From the initial slope of ω_m against κ, we deduce a velocity of 1.05×10^5 cm sec^{-1} for freely propagating shear waves. The arrows shown in Fig. 3

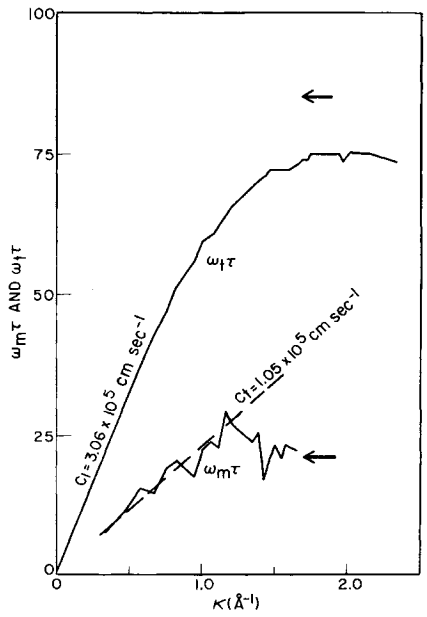

FIG. 5. Relation between ω_m and κ for transverse current fluctuations; velocity of propagation is 1.05×10^5 cm sec^{-1}. Frequency ω_t defined in Eq. (17) is also shown. The square of its slope gives the infinite frequency shear modulus [see Eq. (18)]. The arrows on the right give the positions of the bands shown in Fig. 4.

give an estimate of the reciprocal of the lifetime. Measured in this manner, the lifetimes in units of τ are 0.28, 0.20, and 0.14 for $\kappa = 0.3374$, 0.4771, and 0.5843 Å^{-1}, respectively; note that the lifetime increases essentially as κ^{-1} and not as κ^{-2}, the result expected for density fluctuations in the limit of infinitely long wavelengths.[9]

Note that the straight line indicating the slope of ω_m should not be extrapolated to $\kappa = 0$; at long enough wavelengths, shear waves cannot propagate in a fluid and hence have no velocity of propagation. In the future, molecular-dynamics calculations on much larger systems will certainly allow us to probe longer wavelengths; however, there is no indication from Fig. 3 that we are anywhere near the wavelengths where the spectrum will show, starting from $\omega = 0$, a smooth monotonic decay to zero as ω increases.

B. Response to high frequency shear

From Eq. (16) it follows that

$$\int_{-\infty}^{+\infty} \omega^2 \tilde{C}_\perp(\kappa, \omega)\, d\omega = \omega_t^2 (k_B T/M)\,. \tag{17}$$

This is analogous to Eq. (13) for the second moment of $S(\kappa, \omega)$.

We have shown in the Appendix that in the limit of small κ, ω_t^2 is related to the infinite frequency shear modulus of the system.

$$\lim_{\kappa \to 0} \omega_t^2/\kappa^2 = c_1^2 = G_\infty/d, \tag{18}$$

where d is the mass density and G_∞ is the shear modulus. G_∞ is defined[6] in terms of the frequency-dependent viscosity coefficient, at infinite wavelength $\eta(\omega)$ through the limit

$$G_\infty = \lim_{\omega \to \infty} i\omega\eta(\omega)\,. \tag{19}$$

Figure 5 shows ω_t and leads (since $d = 1$ g cm^{-3}) to $G_\infty = 9.4 \times 10^{10}$ g cm^{-1} sec^{-2}. For liquid argon near the triple point, the value of G_∞ is only $\sim 1.0 \times 10^{10}$ g cm^{-1} sec^{-2}, showing that the hydrogen-bonded water network is one order of magnitude more rigid for shear applied at large frequency.

We do not know of any calculations or experiment for determining G_∞ for ice. One would expect that the high-frequency modulus of rigidity of the solid would be somewhat larger than the value for the liquid.

C. Mean-square force on water molecules

In the Appendix we have shown that

$$\omega_t^2 = \kappa^2 k_B T/M + N^{-1}M^{-1} \times \left\langle \sum_{j=1}^{N} \sum_{l=1}^{N} \left(\frac{\partial^2 U}{\partial x_j \partial x_l} \right) e^{i\kappa(z_j - z_l)} \right\rangle, \tag{A6}$$

where κ is assumed to define the axis z.

We see from Fig. 5 that when $\kappa \approx 2$ Å^{-1}, we have $\omega_t^2 \tau^2 \approx 5625$ and essentially independent of κ. At $\kappa = 2$ Å^{-1}, the kinetic part of $\omega_t^2\tau^2$ [namely, $\tau^2(\kappa^2 k_B T/M)$] is only ≈ 240. This implies that the major contribution to ω_t^2 around $\kappa = 2$ Å^{-1} comes from the potential term in Eq. (A6), and also (because of no dependence on κ) that only the self-term $j = l$ contributes significantly (this being rigorously correct as $\kappa \to \infty$). Hence it is reasonable to write

$$\frac{\tau^2}{M}\left\langle \frac{\partial^2 U}{\partial x^2} \right\rangle \simeq 5625 - 240 = 5385$$

or

$$\frac{\tau^2}{M k_B T}\left\langle \left(\frac{\partial U}{\partial x} \right)^2 \right\rangle \simeq 5385\,.$$

Thus the ratio of the mean-square acceleration $\langle a^2 \rangle$ of a particle to its mean-square velocity $\langle v^2 \rangle$ is

$$\langle a^2 \rangle / \langle v^2 \rangle \simeq 5385\tau^{-2} = 1.184 \times 10^{27} \text{ sec}^{-2}$$

or

$$\langle a^2 \rangle = 1.5 \times 10^{36} \text{ cm}^2 \text{ sec}^{-4}\,.$$

We note in passing that the data published earlier[2] on the velocity autocorrelation of the center of mass of the molecules lead to a value $\langle a^2 \rangle / \langle v^2 \rangle = 1.13 \times 10^{27}$ sec^{-2}.

For comparison, we note that liquid argon near the triple point and also liquid rubidium at 300 °K have $\langle a^2 \rangle \approx 10^{34}$ cm^2 sec^{-4}, a value two orders of magnitude lower. The reason must be that our water model incorporates a stiff hydrogen-bond network that produces large fluctuations in the forces as the network is slowly modified with the passage of time.

The experimental technique to determine $\langle a^2 \rangle$ for structureless molecules makes use of isotopic fractionation for a liquid in equilibrium with its vapor. For monatomic liquids this poses no grave problem. In the case of polyatomic liquids the circumstances are much more involved, owing to the presence of internal degrees of freedom. Moreover, the mean-square torque will also enter into the picture. A mixture of H_2O and D_2O leads to the formation of the intermediate molecule HDO, adding further, perhaps insuperable, difficulties. We suggest, therefore, that isotope-separation experiments should be performed with mixtures of H_2O^{16} and H_2O^{18} for investigating the mean-square force and the mean-square torque on the molecules in the liquid.

VI. SPECTRAL ANALYSIS OF LONGITUDINAL CURRENTS

A. Propagation of density fluctuations (sound waves)

As seen in Fig. 2, $F(\kappa, t)$ is a rather slowly decaying function of time and hence its Fourier transform $S(\kappa, \omega)$ [Eq. (4)] cannot be obtained unless the function is extended to much longer times than shown in Fig. 2. The second time derivative of $F(\kappa, t)$ is proportional to $C_{\parallel}(\kappa, t)$ the longitudinal current fluctuations [Eq. (8)] and Fig. 2 shows that a numerical transform of $C_{\parallel}(\kappa,t)$ is a more feasible procedure to get $S(\kappa, \omega)$ through $\tilde{C}_{\parallel}(\kappa, \omega)$ [Eq. (9)]. However, for the three small values of κ among the five shown in Fig. 2, $C_{\parallel}(\kappa,t)$ is an oscillatory function and one knows that a numerical transform of a truncated oscillatory function leads to spurious oscillations in the spectrum. Hence it is necessary to use an extrapolation procedure even for $C_{\parallel}(\kappa, t)$. For this purpose we will adopt the formalism of the memory-function approach due to Zwanzig[10] (see Ref. 5 for details).

We introduce a new function $M(\kappa, t)$ which satisfies

$$\frac{d}{dt}C_{\parallel}(\kappa, t) = -\omega_0^2\int_0^t C_{\parallel}(\kappa, u)\,du - (\omega_l^2-\omega_0^2)\int_0^t C_{\parallel}(\kappa, u)M(\kappa, t-u)\,du\,. \tag{20}$$

Using the expansion given in Eq. (15), we see that $M(\kappa, 0)=1$. Taking the Laplace transform (denoted by a caret) we get

$$\hat{C}_{\parallel}(\kappa, \epsilon)=\frac{C_{\parallel}(\kappa, t=0)}{\epsilon+\epsilon^{-1}\omega_0^2+(\omega_l^2-\omega_0^2)\hat{M}(\kappa, \epsilon)}\,. \tag{21}$$

Putting $\epsilon=i\omega$ and collecting the real part [which will contain the sine *and* cosine transforms of $M(\kappa, t)$], we get $\pi\tilde{C}_{\parallel}(\kappa, \omega)$, the required function; Eq. (9) then gives $S(\kappa, \omega)$.

The merit of Eq. (20) is that it explicitly incorporates the short-time information about $F(\kappa, t)$ to order t^4 [Eq. (14)] as input—namely, the values of $C_{\parallel}(\kappa, t=0)$, ω_0^2, and ω_l^2—and compacts the rest of the information about $F(\kappa, t)$ into the new function $M(\kappa, t)$, the so-called memory function.

We have used the memory function as a device for extrapolating $C_{\parallel}(\kappa, t)$ to large times by writing

$$M(\kappa, t)=\sum_{n=0}^{m}C_{2n}t^{2n}e^{-\alpha_{2n}t^2}, \tag{22}$$

with $C_0=1$. The parameters α_0, C_2, α_2, ... are used, through Eq. (20), for a least-squares fit with the data for $C_{\parallel}(\kappa, t)$ shown in Fig. 2. Apart from computational facility, there is no particular merit in the above choice of the form of $M(\kappa, t)$. When the memory-function approach to fluctuation phenomena is itself the main theme of investigation, one is required to build the memory function on the basis of physical insight and to consider the reasons why the memory function has a certain structure. In this paper, however, we propose to use $M(\kappa, t)$ only as a computational fitting device.

At $\kappa=0.3374$ Å^{-1}, for example, the data on $C_{\parallel}(\kappa, t)$ shown in Fig. 2 consist of 200 equally spaced points at $\Delta t=\tau/200$ (τ defined in Sec. III). The first 150 of these are used with a seven-parameter (α_0, C_2, α_2, C_4, α_4, C_6, α_6) function $M(\kappa, t)$ for a least-squares fit. The resulting $S(\kappa, \omega)$ is shown in Fig. 6(a). Note that $S(\kappa, \omega)$ has its main intensity around $\omega=0$; this is as expected from Fig. 2, where the area under $F(\kappa, t)$ is obviously seen to be very large. However, the modulation of the slowly decaying $F(\kappa, t)$ is such as to produce an unmistakable "sound" peak at $\omega=12.6\tau^{-1}$, leading to a velocity of propagation $c=\omega/\kappa=1.8\times10^5$ cm sec^{-1}. The width of the peak, however, is so large, and the intensity relative to the central region ($\omega\approx0$) so low, that the fluctuation can hardly be characterized as a freely propagating wave.

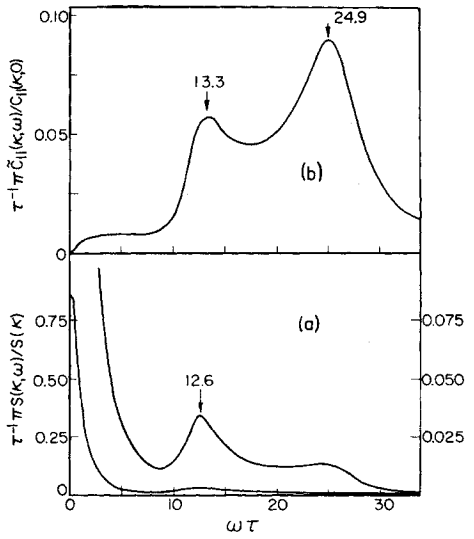

FIG. 6. $S(\kappa, \omega)$, the spectrum of density fluctuations (a) and $\tilde{C}_{\parallel}(\kappa,\omega)$, that of longitudinal currents (b); $\kappa=0.3374$ Å^{-1}. The main peak for sound propagation occurs at $\omega\tau=12.6$. However, considerable intensity persists at $\omega\tau\sim25$. The peaks are clearly seen in $\tilde{C}_{\parallel}(\kappa,\omega)$ since $\tilde{C}_{\parallel}(\kappa,\omega)\propto\omega^2S(\kappa,\omega)$. $S(\kappa,\omega)$ is shown on two different vertical scales for purposes of visibility.

In Fig. 6(a) we see that $S(\kappa, \omega)$ shows noticeable structure again at the larger frequency $\omega \approx 25\tau^{-1}$. This high-frequency structure in $S(\kappa, \omega)$ becomes quite clear in $\tilde{C}_{\parallel}(\kappa, \omega)$, shown in Fig. 6(b). The characteristic frequencies are $\omega = 13.3\tau^{-1}$ and $24.9\tau^{-1}$. In monatomic liquids $\tilde{C}_{\parallel}(\kappa, \omega)$ has always been found to have one peak only which, for κ not too large, is sharp enough to persist as a sound peak in $S(\kappa, \omega)$ when $\tilde{C}_{\parallel}(\kappa, \omega)$ is divided by ω^2. In our model of water we have a clear indication that the current fluctuations have *two* frequencies of major response. At smaller values of κ (not attainable in the present calculation with 216 molecules at a density of 1 g cm^{-3}) we can expect to see two well-defined peaks in $S(\kappa, \omega)$ giving an "ordinary-sound" peak (usually called the Brillouin component of density fluctuations) accompanied by a "high-frequency-sound" peak.

At $\kappa = 0.4771$ Å^{-1} only a suggestion of the low-frequency peak is discernible in $S(\kappa, \omega)$ and $\tilde{C}_{\parallel}(\kappa, \omega)$, as seen in Figs. 7(a) and 7(b). However, the high-frequency peak in $\tilde{C}_{\parallel}(\kappa, \omega)$ clearly occurs at $\omega = 35.0^{-1}$; in Fig. 6(b) this was at $24.9\tau^{-1}$. The ratio 35.0/24.9 is rather close to the ratio 0.4771/0.3374 $= 2^{1/2}$ of the values of κ; thus the high-frequency response in $\tilde{C}_{\parallel}(\kappa, \omega)$ shows normal linear dispersion in going from $\kappa = 0.3374$ to 0.4771 Å^{-1}. The dashed arrow in Fig. 7(a) is drawn at $\omega = 12.6\tau^{-1} \times 2^{1/2} = 17.8\tau^{-1}$; we see the presence of a shoulder in $S(\kappa, \omega)$ at a slightly lower frequency than this value.

Results for $\kappa = 0.6747$ Å^{-1} are shown in Figs. 8(a) and 8(b). The dashed arrows are drawn at frequencies twice as large as those appearing in Figs. 6(a) and 6(b) ($\kappa = 0.3374$ Å^{-1}).

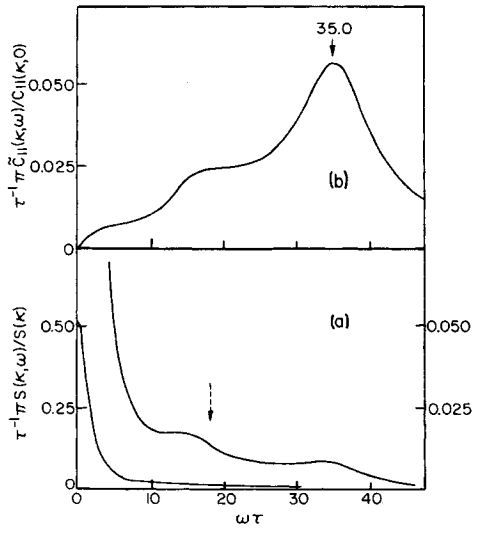

FIG. 7. Same as Fig. 6 but for $\kappa = 0.4771$ Å^{-1}. The dashed arrow is at $\omega\tau = 12.6 \times 0.4771/0.3374$, where a sound peak would be expected in going from $\kappa = 0.3374$ to 0.4771 Å^{-1} if there were no dispersion in the velocity of propagation.

It is clear from the disparity between the positions of the dashed arrows and the shoulders and peaks in the respective spectra that as κ increases the frequencies of maximum response are showing a normal type of dispersive behavior.

It is also clear that we are dealing with wavelengths such that, even for the largest, the collective coordinate is barely propagating and becomes less so for the others.

At high values of κ, as the collective aspect of the coordinate $J_{\parallel}(\kappa, t)$ becomes less marked, the spectrum $\tilde{C}_{\parallel}(\kappa, \omega)$ tends to become independent of κ and similar to $\tilde{C}_{\perp}(\kappa, \omega)$ (see Fig. 5, thick arrows).

B. Short-time behavior of the longitudinal current fluctuation

From Eq. (15) it follows that

$$\int_{-\infty}^{+\infty} \omega^2 \tilde{C}_{\parallel}(\kappa, \omega)\, d\omega = \omega_l^2 (k_B T/M)\,. \tag{23}$$

This is analogous to Eq. (13) for the second moment of $S(\kappa, \omega)$. We have seen in Sec. V that ω_t^2, the second moment of $\tilde{C}_{\perp}(\kappa, \omega)$, is related to the high-frequency shear modulus at infinite wavelength. In systems with two-body central forces, the relation of ω_l^2 to the high-frequency bulk modulus has been demonstrated in the literature. We have *not* found a corresponding relation in the case of two-body noncentral forces, which is the case in our water interaction.

We shall first state the relation of ω_l^2 to G_∞ and κ_∞, the high-frequency shear and bulk moduli, re-

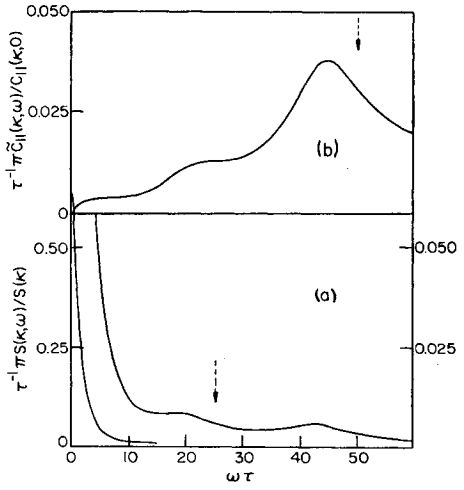

FIG. 8. Same as Figs. 6 and 7, for $\kappa = 0.6747$ Å^{-1}.

spectively, in systems with two-body central forces.[6,7] Let

$$\lim_{\kappa\to\infty}\omega_l^2/\kappa^2 = C_3^2 . \tag{24}$$

Then we have, for mass density d,

$$C_3^2 = (\tfrac{4}{3}G_\infty + K_\infty)/d . \tag{25}$$

Thus in this special case ω_l^2 and ω_t^2, in the limit $\kappa \to 0$, determine G_∞ and K_∞.

In Fig. 9 we have shown ω_l as a function of κ; it is seen that in the water model we have $C_3^2 = 22.09 \times 10^{10}$ cm^2 sec^{-2}.

In the absence of a rigorous relation between C_3^2 and the two moduli, we shall, tentatively, express C_3^2 in the form given above (which is correct for central forces) to derive "K_∞" $= 9.57 \times 10^{10}$ g cm^{-1} sec^{-2}.

For a Lennard-Jones liquid near the triple point, and presumably for liquid argon as well,[11] $K_\infty/G_\infty \approx 1.6$, whereas the values of "K_∞" and G_∞ obtained for water are very nearly the same. There is no reason to believe that the quantity denoted above as K_∞ is the infinite-frequencey bulk modulus in the model of water with which we are concerned. It is to be expected, however, that in the stiff network formed by the hydrogen bonds between molecules which are spatially not well packed (coordination number ≈ 4 and not ≈ 12), K_∞/G_∞ would be less than its value in a monatomic liquid.

Apart from ω_l, Fig. 9 also shows the frequency of the main high-frequency peak in $\tilde{C}_\parallel(\kappa,\omega)$ (marked as ω_m) and the one value (marked as a circle) of the frequency which stands out unambiguously in $S(\kappa,\omega)$ at $\kappa = 0.3774$ Å^{-1} [Fig. 6(a)]. The variation of ω_m with κ gives a "high-frequency-sound" velocity of 3.5×10^5 cm sec^{-1}.

VII. CONCLUDING REMARKS

A system of 216 water molecules packed at a density of 1 g cm^{-3} in a cubic box of side L, with periodic boundary conditions, does not permit the study of phenomena with wavelength greater than L. Hence in the above report the lowest value of κ is $2\pi/L = 0.3374$ Å^{-1}. Our calculations show that at this value of κ there is a fairly well-defined Brillouin peak in the spectrum of density fluctuations giving a sound velocity of 1.8×10^5 cm sec^{-1}. In laboratory experiments with water, at 10 °C, a velocity of 1.5×10^5 cm sec^{-1} is obtained. We conclude that our computer model of liquid water is able to simulate the phenomenon of density fluctuations with considerable fidelity. However, at smaller wavelengths the calculations show only marginal evidence for the existence and propagation of these fluctuations. Hence a calculation with a larger system is called for, and we are presently undertaking such a calculation on 1728 molecules; one cannot but mention that this larger system taxes the available computational resources to a considerable extent.

The overall philosophy behind the technique of molecular dynamics, applied to a phenomenon as complicated as liquid water, should be the achievement of reasonably good agreement with the experimental values of several static and dynamic properties. Given such agreement, if the calculations, in addition, provide evidence of subtle, hitherto unsuspected, properties, it can be considered worthwhile to direct experimental effort towards such properties. An example of this is the presence of high-frequency sound waves with a velocity almost twice that of ordinary sound. We would like to suggest that neutron inelastic scattering experiments on D_2O water at $\kappa \lesssim 0.3$ Å^{-1} covering an energy-transfer range up to 6 meV should be able to register the effects of such waves if they exist.

From Figs. 3 and 6 one can see that the ratio of the low-frequency response in $\tilde{C}_\parallel(\kappa,\omega)$ [corresponding to the ordinary sound peak in $S(\kappa,\omega)$] and the frequency of maximum response in $\tilde{C}_\perp(\kappa,\omega)$ is $13.3/6.6 \approx 2$. This should be compared with the ratio of longitudinal and transverse sound velocities in polycrystalline ice, which is also very

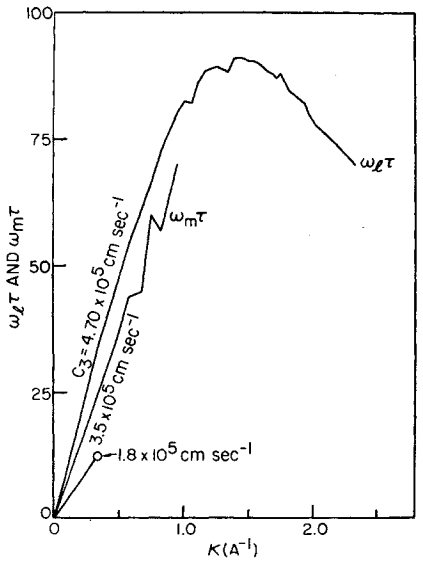

FIG. 9. Circle shows the frequency $\omega \equiv 12.6\tau^{-1}$ (from Fig. 6) plotted against κ. The shoulders in Figs. 7 and 8 are not distinct enough for picking out a clear frequency of response. Tentatively, one may conclude that the molecular-dynamics model suggests a velocity of sound of 1.8×10^5 cm/sec. ω_m is the frequency at which $\tilde{C}_\parallel(\kappa,\omega)$ is maximum for various κ. ω_l is a frequency related to the fourth frequency moment of $S(\kappa,\omega)$; see Eqs. (14) and (15). Its slope is indicated as C_3.

nearly 2.[12] This is further evidence that the molecular-dynamics simulation is indeed close to a real-water system. We should remark here that molecular dynamics is the only technique we know of which can be used to study the behavior of transverse-momentum current fluctuations in liquids; hence, there is no possibility of comparing our results on transverse currents with data from the laboratory. Data from experiments on the solid (in this case ice) is the only comparison possible. Of course, it will be useful to have molecular-dynamics data on ice itself; this is one of the calculations being planned for the future.

The lattice dynamics of ice has been considered by Forslind[13]; he used a dynamical matrix constructed on the basis of the motion of the oxygens alone which interact only with their first neighbors; the elastic-moduli data were then used to determine the force constants and the dynamical matrix solved for the normal modes and their frequencies. The dispersion curves were determined only for vectors $\vec{\kappa}$ in and normal to the hexagonal plane. This work is mentioned here only to point out that the range of the calculated frequencies (12 for each vector $\vec{\kappa}$) extends from zero to 5×10^{13} sec^{-1}, which is precisely the overall range of frequencies that occur in the molecular-dynamics model of water.

APPENDIX

Assuming, without loss of generality, that the wave vector $\vec{\kappa}$ of magnitude κ is in the z direction, we get from Eq. (5),

$$J_\perp = N^{-1/2}\sum_j v_j^x e^{i\kappa z_j}\ , \tag{A1}$$

$$\dot{J}_\perp = N^{-1/2}\sum_j (a_j^x + i\kappa v_j^x v_j^z)e^{i\kappa z_j}\ , \tag{A2}$$

where v_j^x and a_j^x are the x components of the velocity and acceleration of the CM of molecule j.

From Eq. (16) we have

$$\langle |J_\perp|^2\rangle = k_B T/M. \tag{A3}$$

Now $\langle |\dot{J}_\perp|^2\rangle$ has cross terms containing two velocities in normal directions and these terms average to zero. This gives

$$\langle |\dot{J}_\perp|^2\rangle = \left\langle N^{-1}\sum\sum a_j^x a_l^x e^{i\kappa(z_j-z_l)}\right\rangle + \left\langle \kappa^2 N^{-1}\sum\sum v_j^x v_j^z v_l^x v_l^z e^{i\kappa(z_j-z_l)}\right\rangle . \tag{A4}$$

If U denotes the potential energy of the system, Eq. (A4) becomes

$$\langle |\dot{J}_\perp|^2\rangle = k_B T/M^2 N \times\left\langle \sum\sum \frac{\partial^2 U}{\partial x_j \partial x_l} e^{i\kappa(z_j-z_l)}\right\rangle + \kappa^2 (k_B T/M)^2 . \tag{A5}$$

Hence, by the definition of ω_t^2 in Eq. (16),

$$\omega_t^2 = \kappa^2(k_B T/M) + N^{-1}M^{-1} \times\left\langle \sum\sum \frac{\partial^2 U}{\partial x_j \partial x_l} e^{i\kappa(z_j-z_l)}\right\rangle . \tag{A6}$$

In the limit $\kappa \to 0$ we get

$$\omega_t^2 = \kappa^2 c_1^2, \tag{A7}$$

where

$$Mc_1^2 = k_B T - \frac{1}{2N}\left\langle \sum\sum \frac{\partial^2 U}{\partial x_j \partial x_l}(z_j - z_l)^2\right\rangle . \tag{A8}$$

We note that Eq. (34) of Zwanzig and Mountain[6] is applicable to general forces, and by comparison with Eq. (A8) we see that

$$c_1^2 = G_\infty/d .$$

However, in the case of general forces we have not been able to prove a similar result for the longitudinal currents. The case of central forces has been treated by Zwanzig and Mountain[6] and by Zwanzig.[7]

---

*Work performed in part under the auspices of the U. S. Atomic Energy Commission.

[1]This initial study has been referred to and commented upon in Ref. 2.

[2]F. H. Stillinger and A. Rahman, J. Chem. Phys. 60, 1545 (1974).

[3]A. Rahman and F. H. Stillinger, J. Am. Chem. Soc. 95, 7943 (1973).

[4]F. H. Stillinger and A. Rahman, in Proceedings of the Twenty-Fourth International Meeting of the Société de Chimie Physique, Paris, 1973 (unpublished).

[5]A. Rahman, in *Statistical Mechanics, New Concepts, Problems, Applications*, edited by S. A. Rice, K. F. Freed, and J. C. Light (University of Chicago Press, Chicago, 1972).

[6]R. Zwanzig and R. D. Mountain, J. Chem. Phys. 43, 4464 (1965).

[7]R. Zwanzig, Phys. Rev. 156, 190 (1967).

[8]A suitable length parameter for such a comparison is the first-neighbor distance R. In liquid argon near the triple point, this is about 4 Å and in our water model (Fig. 5, Ref. 2) about 3 Å. Thus at values of $R\kappa \approx 1$, water and argon behave rather differently from the point of view in discussion.

[9]A. Rahman, Phys. Rev. Lett. 32, 52 (1974). In this simulation of liquid rubidium a similar phenomenon was observed for the widths of the Brillouin peaks in the spectrum of density fluctuations in the liquid.
[10]R. Zwanzig, in *Lectures in Theoretical Physics*, edited by W. E. Brittin (Wiley, New York, 1961).
[11]D. Levesque, L. Verlet, and J. Kürkijarvi, Phys. Rev. A 7, 1690 (1973).
[12]The data are reviewed by N. E. Dorsey, in *Properties of Ordinary Water-Substance* (Hafner, New York, 1968), p. 461.
[13]E. Forslind, Swedish Cement and Concrete Research Institute at the Royal Institute of Technology, Stockholm, Proceedings No. 21, 1954 (unpublished).